Archive of Numerical Software
vol. 1, no. 1, pages 1–19

Solving Monolithic Fluid-Structure Interaction Problems in Arbitrary Lagrangian Eulerian Coordinates with the deal.II Library

Thomas Wick*[1]

[1]Institute for Applied Mathematics, Heidelberg University

Received: May 22nd, 2011; **final revision:** February 8th, 2012; **published:** May 13th, 2013.

Abstract: We describe a setting of a nonlinear fluid-structure interaction problem and the corresponding solution process in the finite element software package deal.II. The fluid equations are transformed via the ALE mapping (Arbitrary Lagrangian Eulerian framework) to a reference configuration and these are coupled with the structure equations by a monolithic solution algorithm. To construct the ALE mapping, we use a biharmonic equation. Finite differences are used for temporal discretization. The derivation is realized in a general manner that serves for different time stepping schemes. Spatial discretization is based on a Galerkin finite element scheme. The nonlinear system is solved by a Newton method. Using this approach, the Jacobian matrix is constructed by exact computation of the directional derivatives. The implementation using the software library package deal.II serves for the computation of different fluid-structure configurations. Specifically, our geometry data are taken from the fluid-structure benchmark configuration that was proposed in 2006 in the *DFG project Fluid-Structure Interaction I: Modelling, Simulation, Optimisation*. Our results show that this implementation using deal.II is able to produce comparable findings.

1 Introduction

Fluid-structure interactions occur in many situations in industry and biomedical engineering (Jianhai et al., 2006; Piperno and Farhat, 2001; Tallec and Mouro, 2001; Figueroa et al., 2006; Santos et al., 2008; Nobile and Vergara, 2008; Vierendeels et al., 2008). Typically, the fluid and the structure equations are modeled in different coordinate systems making a common solution approach challenging. Fluid flows are modeled in an Eulerian framework whereas the structure is treated in Lagrangian coordinates. In this work, we use a monolithic approach in which all equations are solved simultaneously (Hron, 2001; Hron and Turek, 2006; Fernández and Gerbeau, 2009; Bungartz and Schäfer, 2006; Richter and Wick, 2010; Bungartz et al., 2010; Wick, 2011) and the many references cited therein. Employing this approach, the interface conditions, the continuity of velocity and the normal stresses, are automatically achieved at each time step (*strongly coupled approach* (Fernández and Gerbeau, 2009; Wall et al., 2007; Matthies et al., 2006; Tezduyar et al.,

*thomas.wick@iwr.uni-heidelberg.de

2006)). The coupling leads to additional nonlinear behavior of the overall system. However, a strong coupling can also be achieved by solving the two systems iteratively (for an brief overview, we refer the reader to (Fernández and Gerbeau, 2009)). In such settings, the problem is seen as a non-overlapping domain decomposition method (Küttler and Wall, 2008; Mok and Wall, 2001; Deparis et al., 2006). In such a system, the coupling can be treated as Dirichlet-Neumann coupling, which is subject of a discussion in (Küttler and Wall, 2008) or leading to an approach in which the whole problem is reduced to only solving interface variables (Deparis et al., 2006).

Using a monolithic formulation is motivated by three issues. First, a coupled monolithic variational formulation is an inevitable prerequisite for gradient based optimization methods (Becker et al., 2000), for rigorous goal oriented error estimation and mesh adaptation (Becker and Rannacher, 2001). The latter issue has already been investigated for stationary fluid-structure interaction settings in (van der Zee et al., 2008; Richter, 2012; Wick, 2012). In addition, the programming code serves for the modeling and simulation of bio-medical applications in hemodynamics (Wick, 2011). Here, the densities of the blood and the vessels walls are of the same order, leading to the so-called 'added-mass' effect (Causin et al., 2005). This artefact causes numerical instabilities when using partitioned solution algorithms.

For fluid-structure interaction based on the 'arbitrary Lagrangian-Eulerian' (ALE) frame of reference, the choice of appropriate fluid mesh movement is important. We emphasize that the ALE framework is a standard framework nowadays to solving fluid-structure interactions (Donéa et al., 1977; Ghattas and Li, 1995; Hirt et al., 1974; Hughes et al., 1981). The crucial issue in this framework is the construction of the fluid mesh motion. In this study, we use the biharmonic operator (in a mixed formulation) for the mesh motion. It has the advantage to enable large deformations of the structure but has increased computational cost (Helenbrook, 2001; Wick, 2011). These ingredients lead to a solvable semi-linear form of the coupled setting on the continuous level.

Afterwards, we discretize this setting. Temporal discretization is based on finite differences and a formulation as one step-θ scheme (see, e.g., (Turek, 1999)), from which we can extract the implicit Euler, Crank-Nicolson, and the shifted Crank-Nicolson scheme.

Spatial discretization is realized by a standard Galerkin finite element approach by using the Q_2^c/P_1^{dc} element for fluid flows and Q_2^c for structural discretization (Girault and Raviart, 1986). The solution of the nonlinear discretized system can be achieved with a Newton method, which is very attractive because it provides robust and rapid convergence. The Jacobian matrix is derived by exact linearization (Fernández and Moubachir, 2005) that is demonstrated by an example. A very detailed consideration is undertaken in (Wick, 2011). Because the development of preconditioners for iterative linear solvers is difficult for fully coupled problems (however, suggestions have been made (Heil, 2004; Badia et al., 2008; Richter, 2010)), we use a direct solver (UMFPACK Davis and Duff (1997)) to solve the linear systems. Nevertheless, we extract the block-structure to clearify the inner sub-structure of the system matrix (Jacobian). This knowledge facilitates the development of a preconditioner that is based on a Block-Schur complement iteration.

In the last section, we consider three numerical examples that are taken from (Bungartz and Schäfer, 2006). The provided programming code is able to reproduce these results and is based on the finite element software library deal.II (Bangerth et al., 2012).

The outline of this paper is as follows. In Section 2, we introduce the equations for the fluid and the structure and their coupling in a monolithic fashion. In Section 3, the discretization and the linearization of the unsteady nonlinear problem are subject of our discussion. After these considerations, we extract the inner structure of the system matrix. In the last section, we discuss three results that are motivated by the fluid-structure benchmark computations and which are derived with the accompanying source code. In the appendices, we describe how to run the provided source code and we give a brief explication of the features of the source code.

2 Equations in Variational Formulation

We denote by $\Omega \subset \mathbb{R}^d, d = 2, 3$, the domain of the fluid-structure interaction problem. This domain is supposed to be time independent but consists of two time dependent subdomains $\Omega_f(t)$ and $\Omega_s(t)$. The interface between both domains is denoted by $\Gamma_i(t) = \partial\Omega_f(t) \cap \partial\Omega_s(t)$. The initial (i.e., the reference) domains are denoted by $\widehat{\Omega}_f$ and $\widehat{\Omega}_s$, respectively, with their common interface $\widehat{\Gamma}_i$. Furthermore, we denote the outer boundary with $\partial\widehat{\Omega} = \widehat{\Gamma} = \widehat{\Gamma}_D \cup \widehat{\Gamma}_N$ where $\widehat{\Gamma}_D$ and $\widehat{\Gamma}_N$ denote Dirichlet and Neumann boundaries, respectively.

We adopt standard notation for the usual Lebesgue and Sobolev spaces (Wloka, 1982). We use the notation $(\cdot,\cdot)_X$ for a scalar product on a Hilbert space X and $\langle\cdot,\cdot\rangle_{\partial X}$ for the scalar product on the boundary ∂X. We indicate by $L^p(X), 1 \le p \le \infty$ the standard Lebesgue space that consists of measurable functions u, which are Lebesgue-integrable to the p-th power. The set $L^p(X)$ forms a Banach space with the norm $\|u\|_{L^p(X)}$. For $p = 2, H^m(X) := W^{m,2}(X)$ is a Hilbert space equipped with the norm $\|\cdot\|_{H^m(X)}$ (Wloka, 1982). Finally, we indicate the subspace $W^{m,p}(X)$ of functions with zero trace on ∂X by $W_0^{m,p}(X)$. Specifically, we define $H_0^1(X) = \{u \in H^1(X) : \ u = 0 \text{ on } \Gamma_D \subset \partial X\}$. We use frequently the short notation

$$\hat{\mathcal{V}} := H^1(X), \quad \hat{\mathcal{V}}^0 := H_0^1(X),$$

and

$$\hat{\mathcal{L}} := L^2(X), \quad \hat{\mathcal{L}}^0 := L^2(X)/\mathbb{R}.$$

2.1 The coupled problem on the continuous level

In this work, the interaction of an incompressible Newtonian fluid and an elastic structure of hyperbolic type is studied. The equations for fluid and structure are defined in their natural frameworks. In the fluid problem, we aim to find a vector-valued velocity v and scalar-valued pressure such that:

$$\begin{aligned} \rho_f \, \partial_t v_f\big|_{\hat{\mathcal{A}}} + \rho_f(v_f - \partial_t u_f)\cdot\nabla v_f - \mathrm{div}\sigma_f = 0 \quad &\text{in } \Omega_f(t), \\ \mathrm{div} v_f = 0 \quad &\text{in } \Omega_f(t), \\ v_f = v^D \quad \text{on } \Gamma_{f,\mathrm{in}}(t), \quad \sigma n_f = g_{f,N} \quad &\text{on } \Gamma_{f,N}(t), \end{aligned} \tag{1}$$

with the Cauchy stress tensor σ_f. With the help of the (undamped) structure problem, we aim to find a vector-valued displacement $\hat{u}$ such that:

$$\begin{aligned} \hat{\rho}_s\partial_t^2\hat{u}_s - \widehat{\mathrm{div}}(\widehat{F\Sigma}_s) = 0 \quad &\text{in } \widehat{\Omega}_s, \\ \hat{u}_f = 0 \quad \text{on } \widehat{\Gamma}_{s,D}, \quad \widehat{F\Sigma}_s\hat{n}_s = 0 \quad &\text{on } \widehat{\Gamma}_{s,N}, \end{aligned} \tag{2}$$

with the second Piola-Kirchhoff tensor $\widehat{\Sigma}_s$ and the deformation gradient $\widehat{F} = I + \widehat{\nabla}\hat{u}$, where I denotes the identity tensor. The coupling conditions are given by (with $\det(\widehat{F}) = J$):

$$v_f = \partial_t u_f \ \text{ on } \Gamma_i(t), \quad \widehat{F\Sigma}_s n_s + \widehat{J\sigma F^{-T}}\hat{n}_f = 0 \ \text{ on } \widehat{\Gamma}_i, \tag{3}$$

where $\partial_t\hat{u}_f$ denotes the fluid domain velocity that satisfies $\partial_t\hat{u}_f = \hat{v}_s$ on $\widehat{\Gamma}_i$. The stress tensors, σ_f and $\widehat{\Sigma}_s$, are defined by

$$\begin{aligned} \sigma_f &:= -p_f I + \rho_f\nu_f(\nabla v_f + \nabla v_f^T), \\ \widehat{\Sigma}_s &:= (\lambda_s(\mathrm{tr}\widehat{E})I + 2\mu_s\widehat{E}), \quad \widehat{E} = \frac{1}{2}(\widehat{F}^T\widehat{F} - I). \end{aligned}$$

The viscosity and the density of the fluid are denoted by ν_f and ρ_f, respectively. The elastic (combressible) structure is characterized by the Lamé coefficients μ_s, λ_s.

The principal unknowns are the fluid velocity $\hat{v}_f : \widehat{\Omega}_f \times R^+ \to R^3$, the fluid pressure $\hat{p} : \widehat{\Omega}_f \times R^+ \to R$, the structure displacement $\hat{u}_s : \widehat{\Omega}_s \times R^+ \to R^3$, and the fluid domain displacement (mesh motion) $\hat{u}_f : \widehat{\Omega}_f \times R^+ \to R^3$. The ALE mapping is denoted by $\hat{\mathcal{A}}$ and transforms the reference configuration $\widehat{\Omega}_f$ of the fluid to the physical domain $\Omega_f(t)$. This mapping is defined through the extension of the structural displacement into the fluid domain; thus $\hat{u}_f = \text{Ext}(\hat{u}_s|_{\widehat{\Gamma}_i})$ and solving an additional partial differential equation that is given in Section 2.2. Furthermore, any function $\hat{q} \in \widehat{\Omega}$ can be defined Ω by $q(x) = \hat{q}(\hat{x})$ with $x = \hat{\mathcal{A}}(\hat{x}, t)$.

2.2 Construction of the ALE mapping

The fluid domain motion is constructed by posing an auxiliary equation, which is driven by the motion of the interface $\Gamma_i(t)$, i.e., $\hat{\mathcal{A}} = \hat{u}_s$ on $\widehat{\Gamma}_i$, leading to $\partial_t \hat{u}_f = \hat{v}_s$ on $\widehat{\Gamma}_i$. Furthermore, we fix all outer boundaries of the domain by $\hat{u}_f = 0$. In the fluid domain $\widehat{\Omega}_f$, the transformation $\hat{\mathcal{A}}$ is arbitrary but should satisfy certain regularity conditions (C^1-diffeomorphism). Specifically, the fluid mesh is constructed by solving a biharmonic equation (for large mesh deformations without re-meshing):

$$\begin{aligned} \Delta^2 \hat{u}_f &= 0 \quad \text{in } \widehat{\Omega}_f, \\ \hat{u}_f = \partial_n \hat{u}_f &= 0 \quad \text{on } \widehat{\Gamma}_{f,\text{in}} \cup \widehat{\Gamma}_{f,\text{out}}, \\ \hat{u}_f = \hat{u}_s \quad &\text{and} \quad \partial_n \hat{u}_f = \partial_n \hat{u}_s \quad \text{on } \widehat{\Gamma}_i. \end{aligned}$$

The ALE map is constructed by solving a mixed formulation of the biharmonic equation in the sense of Ciarlet (Ciarlet and Raviart, 1974). We introduce an auxiliary variable $\hat{w} = -\hat{\Delta}\hat{u}$ and obtain two differential equations:

$$\begin{aligned} \hat{w} &= -\hat{\Delta}\hat{u} \qquad \text{in } \widehat{\Omega}, \\ -\hat{\Delta}\hat{w} &= 0 \qquad \text{in } \widehat{\Omega}_f. \end{aligned} \tag{4}$$

with the boundary conditions

$$\begin{aligned} \hat{u}_f = \partial_n \hat{u}_f &= 0 \quad \text{on } \widehat{\Gamma}_{f,\text{in}} \cup \widehat{\Gamma}_{f,\text{out}}, \\ \hat{u}_f = \hat{u}_s \quad &\text{and} \quad \partial_n \hat{u}_f = \partial_n \hat{u}_s \quad \text{on } \widehat{\Gamma}_i. \end{aligned}$$

2.3 The variational system in the reference configuration

Until now, the description of the coupled problem serves for partitioned and monolithic solution algorithms. In the following, we concentrate on a monolithic description of the coupled problem. Specifically, the fluid equations are transformed to a fixed reference configuration and is solved therein. A continuous variable $\hat{u}$ in $\widehat{\Omega}$, defining the deformation in $\widehat{\Omega}_s$, and supporting the transformation in $\widehat{\Omega}_f$ is defined. Then, we get the standard relations

$$\hat{\mathcal{A}} := \text{id} + \hat{u}, \quad \widehat{F} := I + \hat{\nabla}\hat{u}, \quad \hat{J} := \det(\widehat{F}). \tag{5}$$

Furthermore, the velocity $\hat{v}$ is a common continuous function for both subproblems, whereas the pressure $\hat{p}$ is discontinuous. We state the monolithic setting for fluid-structure interaction with a biharmonic mesh motion model:

Problem 2.1 (Variational fluid-structure interaction, biharmonic mesh motion) *Find* $\{\hat{v}, \hat{u}, \hat{w}, \hat{p}\} \in \{\hat{v}^D + \hat{\mathcal{V}}^0\} \times \{\hat{u}^D + \hat{\mathcal{V}}^0\} \times \hat{\mathcal{V}} \times \hat{\mathcal{L}}$, *such that* $\hat{v}(0) = \hat{v}^0$ *and* $\hat{u}(0) = \hat{u}^0$, *for almost all* $t \in I$, *and*

$$
\begin{aligned}
(\hat{J}\hat{\rho}_f \partial_t \hat{v}, \hat{\psi}^v)_{\widehat{\Omega}_f} + (\hat{\rho}_f \hat{J}(\widehat{F}^{-1}(\hat{v} - \partial_t \hat{u}_f) \cdot \widehat{\nabla})\hat{v}), \hat{\psi}^v)_{\widehat{\Omega}_f} \\
+(\hat{J}\widehat{\sigma}_f \widehat{F}^{-T}, \widehat{\nabla}\hat{\psi}^v)_{\widehat{\Omega}_f} + (\hat{\rho}_s \partial_t \hat{v}, \hat{\psi}^v)_{\widehat{\Omega}_s} + (\widehat{F\Sigma}_s, \widehat{\nabla}\hat{\psi}^v)_{\widehat{\Omega}_s} - \langle \hat{g}, \hat{\psi}^v \rangle_{\widehat{\Gamma}_{out}} = 0 \quad \forall \hat{\psi}^v \in \hat{\mathcal{V}}^0, \\
(\partial_t \hat{u} - \hat{v}, \hat{\psi}^u)_{\widehat{\Omega}_s} + (\hat{\alpha}_w \widehat{\nabla}\hat{w}, \widehat{\nabla}\hat{\psi}^u)_{\widehat{\Omega}_f} - \langle \hat{\alpha}_w \hat{n}_f \widehat{\nabla}\hat{w}, \hat{\psi}^u \rangle_{\widehat{\Gamma}_i} = 0 \quad \forall \hat{\psi}^u \in \hat{\mathcal{V}}^0, \\
(\hat{\alpha}_u \hat{w}, \hat{\psi}^w)_{\widehat{\Omega}} + (\hat{\alpha}_u \widehat{\nabla}\hat{u}, \widehat{\nabla}\hat{\psi}^w)_{\widehat{\Omega}} - \langle \hat{\alpha}_u \hat{n}_f \widehat{\nabla}\hat{u}, \hat{\psi}^w \rangle_{\widehat{\Gamma}_i} = 0 \quad \forall \hat{\psi}^w \in \hat{\mathcal{V}}, \\
(\widehat{div}(\hat{J}\widehat{F}^{-1}\hat{v}), \hat{\psi}^p)_{\widehat{\Omega}_f} = 0 \quad \forall \hat{\psi}^p \in \hat{\mathcal{L}},
\end{aligned}
$$

with $\hat{\rho}_f$, $\hat{\rho}_s$, ν_f, μ_s, λ_s, $\widehat{F}$, $\hat{J}$, *and positive diffusion parameters* $\hat{\alpha}_u$ *and* $\hat{\alpha}_w$. *The stress tensors,* $\hat{\sigma}_f$ *and* $\hat{\sigma}_s$, *are defined as*

$$
\begin{aligned}
\widehat{\sigma}_f &:= -\hat{p}_f I + \hat{\rho}_f \nu_f (\widehat{\nabla}\hat{v}\widehat{F}^{-1} + \widehat{F}^{-T}\widehat{\nabla}\hat{v}^T), \\
\widehat{\Sigma}_s &:= \lambda_s (tr\widehat{E}) I + 2\mu_s \widehat{E}.
\end{aligned}
$$

The viscosity and the density of the fluid are denoted by ν_f *and* $\hat{\rho}_f$, *respectively. The function* $\hat{g}$ *represents Neumann boundary conditions on the outflow boundary. Specifically, we have* $\hat{g} := \hat{\rho}_f \nu_f \hat{J}(\widehat{F}^{-T}\widehat{\nabla}\hat{v})\widehat{F}^{-T}$ *on* $\widehat{\Gamma}_{out}$ *(see Figure 1). The structure is characterized by the density* $\hat{\rho}_s$, *the Lamé coefficients* μ_s, λ_s. *For the STVK material, the compressibility is related to the Poisson ratio* ν_s ($\nu_s < \frac{1}{2}$).

The Problem 2.1 is completed by an appropriate choice of the two coupling conditions on the interface. The continuity of velocity across $\hat{\Gamma}_i$ is strongly enforced by requiring one common continuous velocity field on the whole domain $\hat{\Omega}$. The continuity of normal stresses is given by

$$
(\hat{J}\widehat{\sigma}_s \widehat{F}^{-T}\hat{n}_s, \hat{\psi}^v)_{\widehat{\Gamma}_i} = (\hat{J}\widehat{\sigma}_f \widehat{F}^{-T}\hat{n}_f, \hat{\psi}^v)_{\widehat{\Gamma}_i}. \tag{6}
$$

By omitting this boundary integral jump over $\widehat{\Gamma}_i$ the weak continuity of the normal stresses becomes an implicit condition of the fluid-structure interaction problem.

Remark 2.1 *The boundary terms on* $\widehat{\Gamma}_i$ *in the Problem 2.1 are necessary to prevent spurious feedback of the displacement variables* $\hat{u}$ *and* $\hat{w}$. *A discussion on this subject is made in (Richter and Wick, 2010). However, we performed numerical experiments (that will be not discussed in this work) to study the influence of these terms. Our findings suggest to neglict these terms. Nevertheless, we provide the implementation in the source code such that we are able to test the switch between usage or not of these terms.*

3 Discrete Level

In this section, we briefly comment on temporal and spatial discretization and explain the solution process of the nonlinear problem. Finally, we give a short account on the form of the linear equation system, which must be solved in each Newton step. In fact, because that the fluid equations have been transformed on a fixed reference configuration, the whole problem is solved therein (instead of moving the fluid mesh explicitly).

3.1 Temporal and spatial discretization

The continuous problem is treated with the Rothe method, thus, first discretizing in time and afterwards in space. Therefore, a semi-linear form is introduced and the problem 2.1 is written in compact notation: Find $\hat{U} = \{\hat{v}, \hat{u}, \hat{w}, \hat{p}\} \in \hat{X}$, where $\hat{X}^0 := \{\hat{v}^D + \hat{\mathcal{V}}^0\} \times \{\hat{u}^D + \hat{\mathcal{V}}^0\} \times \hat{\mathcal{V}} \times \hat{\mathcal{L}}$, such that

$$
\int_0^T \hat{A}(\hat{U})(\hat{\Psi})\, dt = 0 \quad \forall \hat{\Psi} \in \hat{X}^0. \tag{7}
$$

The time integral is defined in an abstract sense such that the equation holds for *almost* all time steps. The semi-linear form $\hat{A}(\hat{U})(\hat{\Psi})$ is defined by

$$\begin{aligned}\hat{A}(\hat{U})(\hat{\Psi}) &= (\hat{J}\hat{\rho}_f\partial_t\hat{v},\hat{\psi}^v)_{\widehat{\Omega}_f} + (\hat{\rho}_f\hat{J}(\widehat{F^{-1}}(\hat{v}-\partial_t\hat{u}_f)\cdot\widehat{\nabla})\hat{v}),\hat{\psi}^v)_{\widehat{\Omega}_f}\\ &+ (\widehat{J\sigma_f}\widehat{F^{-T}},\widehat{\nabla}\hat{\psi}^v)_{\widehat{\Omega}_f} + (\hat{\rho}_s\partial_t\hat{v},\hat{\psi}^v)_{\widehat{\Omega}_s} + (\widehat{F\Sigma_s},\widehat{\nabla}\hat{\psi}^v)_{\widehat{\Omega}_s} - \langle\hat{g},\hat{\psi}^v\rangle_{\widehat{\Gamma}_{out}}\\ &+ (\partial_t\hat{u},\hat{\psi}^u)_{\widehat{\Omega}_s} - (\hat{v},\hat{\psi}^u)_{\widehat{\Omega}_s} + (\hat{\alpha}_w\widehat{\nabla}\hat{w},\widehat{\nabla}\hat{\psi}^u)_{\widehat{\Omega}_f} - \langle\hat{\alpha}_w\hat{n}_f\hat{\nabla}\hat{w},\hat{\psi}^u\rangle_{\hat{\Gamma}_i}\\ &+ (\hat{\alpha}_u\hat{w},\hat{\psi}^w)_{\widehat{\Omega}} + (\hat{\alpha}_u\widehat{\nabla}\hat{u},\widehat{\nabla}\hat{\psi}^w)_{\widehat{\Omega}} - \langle\hat{\alpha}_u\hat{n}_f\hat{\nabla}\hat{u},\hat{\psi}^w\rangle_{\hat{\Gamma}_i}\\ &+ (\widehat{\mathrm{div}}\,(\hat{J}\widehat{F^{-1}}\hat{v}),\hat{\psi}^p)_{\widehat{\Omega}_f} \quad \forall\hat{\Psi}\in\hat{X}^0, \end{aligned} \tag{8}$$

with $\hat{\Psi} = \{\hat{\psi}^v,\hat{\psi}^u,\hat{\psi}^w,\hat{\psi}^p\} \in \hat{\mathcal{V}}^0\times\hat{\mathcal{V}}^0\times\hat{\mathcal{V}}\times\hat{\mathcal{L}}$. Temporal discretization is based on finite differences and the one step-θ schemes (Turek, 1999). The derivation for our set of equations was made in (Wick, 2011). A numerical comparison for different type of time-stepping schemes is undertaken in (Wick, 2011). Spatial discretization in the reference configuration $\widehat{\Omega}$ is treated by a conforming Galerkin finite element scheme, leading to a finite dimensional subspace $\hat{X}_h \subset \hat{X}$. The discrete spaces are based on the Q_2^c/P_1^{dc} element for the fluid problem (Girault and Raviart, 1986). The structure problem is discretized by the Q_2^c element. Other (reasonable) choices of finite elements (selected from appropriate functional spaces) might be tested for the present source code.

3.2 Linearization techniques for the nonstationary problem

Time and spatial discretization end at each single time step in a nonlinear quasi-stationary problem

$$\hat{A}(\hat{U}_h^n)(\hat{\Psi}) = \hat{F}(\hat{\Psi}) \quad \forall\hat{\Psi}\in\hat{X}_h,$$

which is solved with a Newton-like method. Given an initial Newton guess $\hat{U}_h^{n,0}$, find for $j = 0,1,2,\ldots$ the update $\delta\hat{U}_h^n$ of the linear defect-correction problem

$$\begin{aligned}\hat{A}'(\hat{U}_h^{n,j})(\delta\hat{U}_h^n,\hat{\Psi}) &= -\hat{A}(\hat{U}_h^{n,j})(\hat{\Psi}) + \widehat{F}(\hat{\Psi}),\\ \hat{U}_h^{n,j+1} &= \hat{U}_h^{n,j} + \lambda\delta\hat{U}_h^n. \end{aligned} \tag{9}$$

In this algorithm, $\lambda\in(0,1]$ is used as damping parameter for line search iterations. A crucial role for (highly) nonlinear problems includes the appropriate determination of λ. A simple strategy is to modify the update step in (9) as follows: For given $\lambda\in(0,1)$ determine the minimal $l^*\in\mathbb{N}$ via $l = 0,1,\ldots,N_l$, such that

$$\begin{aligned}R(\hat{U}_{h,l}^{n,j+1}) &< R(\hat{U}_{h,l}^{n,j}),\\ \hat{U}_{h,l}^{n,j+1} &= \hat{U}_h^{n,j} + \lambda^l\delta\hat{U}_h^n. \end{aligned}$$

For the minimal l, we set

$$\hat{U}_h^{n,j+1} := \hat{U}_{h,l^*}^{n,j+1}.$$

In this context, the nonlinear residual $R(\cdot)$ is defined as

$$R(\hat{U}_h^n) := \max_i\left\{\hat{A}(\hat{U}_h^n)(\hat{\Psi}_i) - \hat{F}(\hat{\Psi}_i)\right\} \quad \forall\hat{U}_h^n\in\hat{X}_h,$$

where $\{\hat{\Psi}_i\}$ denotes the nodal basis of $\hat{X}_h$.

The directional derivative $\hat{A}'(\hat{U})(\delta\hat{U},\hat{\Psi})$ that is utilized previously, is defined as Gâteaux derivative The application to a semi-linear form reads:

$$\hat{A}'(\hat{U})(\delta\hat{U},\hat{\Psi}) := \lim_{\varepsilon\to 0}\frac{1}{\varepsilon}\left\{\hat{A}(\hat{U}+\varepsilon\delta\hat{U})(\hat{\Psi}) - \hat{A}(\hat{U})(\hat{\Psi})\right\} = \frac{d}{d\varepsilon}\,\hat{A}_h(\hat{U}+\varepsilon\delta\hat{U})(\hat{\Psi})\Big|_{\varepsilon=0}.$$

Directional derivatives needed for the Newton method

In this section, we discuss an example of one specific directional derivative that includes all of the necessary steps. We also refer the reader to other discussions on the exact derivation of the Jacobian (Fernández and Moubachir, 2005; Wick, 2011).

Let us consider a part of the fluid convection term in ALE coordinates. As part of a semi-linear form, it holds

$$\hat{A}_{\text{conv}}(\hat{U})(\hat{\Psi}) = (\hat{\rho}_f \hat{J}(\hat{F}^{-1}\hat{v}\cdot\hat{\nabla})\hat{v}, \hat{\psi}^v)_{\hat{\Omega}_f} = (\hat{\rho}_f \hat{\nabla}\hat{v}\, \hat{J}\hat{F}^{-1}\,\hat{v}, \hat{\psi}^v)_{\hat{\Omega}_f}.$$

In this case, the directional derivative $\hat{A}'_{\text{conv}}(\hat{U})(\delta\hat{U}, \hat{\Psi})$ in the direction $\delta\hat{U} = \{\delta\hat{v}, \delta\hat{u}, \delta\hat{p}\}$ is given by

$$\hat{A}'_{\text{conv}}(\hat{U})(\delta\hat{U}, \hat{\Psi}) = \left(\hat{\nabla}\delta\hat{v}\, \hat{J}\hat{F}^{-1}\,\hat{v}, \hat{\psi}^v\right) + \left(\hat{\nabla}\hat{v}\,(\hat{J}\hat{F}^{-1})'(\delta\hat{u})\,\hat{v}, \hat{\psi}^v\right) + \left(\hat{\nabla}\hat{v}\,\hat{J}\hat{F}^{-1}\delta\hat{v}, \hat{\psi}^v\right). \tag{10}$$

In the following, we restrict our considerations to an two-dimensional example because the inverse of the deformation matrix can easily be stated in explicit form. However, the three-dimensional solution of fluid-structure interactions is also possible with our programming code (Wick, 2011). For a more compact notation, we refer the reader to (Wick, 2011). Explicitly, the deformation matrix reads:

$$\hat{F} = I + \hat{\nabla}\hat{u} = \begin{pmatrix} 1+\hat{\partial}_1\hat{u}_1 & \hat{\partial}_2\hat{u}_1 \\ \hat{\partial}_1\hat{u}_2 & 1+\hat{\partial}_2\hat{u}_2 \end{pmatrix},$$

which brings us to

$$\hat{J}\hat{F}^{-1} = \begin{pmatrix} 1+\hat{\partial}_2\hat{u}_2 & -\hat{\partial}_2\hat{u}_1 \\ -\hat{\partial}_1\hat{u}_2 & 1+\hat{\partial}_2\hat{u}_2 \end{pmatrix},$$

and its directional derivative in direction $\delta\hat{u} = (\delta\hat{u}_1, \delta\hat{u}_2)$:

$$(\hat{J}\hat{F}^{-1})'(\delta\hat{u}) = \begin{pmatrix} \hat{\partial}_2\delta\hat{u}_2 & -\hat{\partial}_2\delta\hat{u}_1 \\ -\hat{\partial}_1\delta\hat{u}_2 & \hat{\partial}_2\delta\hat{u}_2 \end{pmatrix}.$$

This expression is part of the second term shown in Equation (10). The remaining expressions for directional derivatives can be derived in an analogous way. For more details on computation of the directional derivatives on the interface, we refer to (Richter and Wick, 2010). With these ingredients the Jacobian is built explicitly (as also done in (Fernández and Moubachir, 2005; Barker and Cai, 2010)) to identity optimal Newton convergence.

3.3 Block-structure of the linear equation system

After discretization and linearization, we solve in each Newton step a linearized problem, to achieve the solution of the (originally) nonlinear problem. The investigation of the block-structure of the linear system was already discussed for a stationary setting with a harmonic fluid mesh-motion model in (Janssen and Wick, 2010). In this work, we upgrade these ideas to the unsteady case and the biharmonic fluid mesh-motion model. Specifically, we are interested in the block-structure of the semi-linear form (8). To ease the notation in this section, we omit the 'hats' because it is clear that we are still working in the reference configuration $\widehat{\Omega}$.

The global linear equation system has the following form in each Newton step (9):

$$\begin{pmatrix} \frac{M_{vv}}{k} + N_{vv} + L_{vv} + \frac{M_{vv}}{k} & E_{vu} + S_{vu} & 0 & B_{vp} \\ M_{uv} & \frac{M_{uu}}{k} & \alpha_w L_{uw} & 0 \\ 0 & \alpha_u L_{wu} & \alpha_u M_{ww} & 0 \\ B_{vp}^T & S_{pu} & 0 & M_{pp} \end{pmatrix} \begin{pmatrix} \delta v \\ \delta u \\ \delta w \\ \delta p \end{pmatrix} = \begin{pmatrix} b_v(t_{n+1}, t_n, u_n) \\ b_u(t_{n+1}, t_n, u_n) \\ b_w(t_{n+1}, t_n, u_n) \\ b_p(t_{n+1}, t_n, u_n) \end{pmatrix}, \tag{11}$$

Here, the introduced matrices are characterized as follows. In the first block, we have in the fluid domain the mass term M_{vv}, the convection term N_{vv}, the Laplacian L_{vv} and a mass matrix M_{vv} in

the structure part. In the next block in the upper row, we find the elasticity of the structure and couplings terms in the fluid domain. In the last block, we have the gradient matrix B_{vp}. In the second row, in the first two blocks, we find again two mass terms M_{uv} and M_{uu} in the structure domain. Then, we detect a Laplacian L_{uw} due to the biharmonic fluid mesh motion. In the third row, we start in the second block with a Laplacian L_{wu} because of the mesh motion model. The same reason holds for the appearance of the next mass term M_{ww}. In the last row, we find the (negative) transposed divergence matrix B_{vp}^T. Then, we have again a coupling term S_{pu} and in the last entry of the system matrix, we have the pressure mass matrix in the structure domain. Except of the diffusion parameters of the mesh motion model and the time step k, we omitted all other parameters. Specifically, the θ parameter of the time-stepping scheme is not shown. We recall, that all terms of the former time step are hidden in the right hand side vector $B = \{b_v, b_u, b_w, b_p\}$. Though, in each Newton step, see equation (9), we are concerned with a linear system

$$A\,\delta U = B, \tag{12}$$

where A denotes a block matrix and $\delta U = \{\delta v, \delta u, \delta w, \delta p\}$ and solution vector. To solve system (12), one could try to find a preconditioner such that

$$P^{-1}A\,\delta U = P^{-1}B. \tag{13}$$

If we find appropriate entries for P^{-1} such that the condition number of $P^{-1}A$ is moderate, then the whole systems would converge in a few iterations. Specifically, we use geometric multigrid method to solve the Laplace-dominated blocks in the preconditioner. This method was introduced in deal.II in (Janssen and Kanschat, 2011).

The representation (11) shadows one important fact. Namely, that all terms are defined on two different domains $\widehat{\Omega}_f$ and $\widehat{\Omega}_s$, which has consequences for an appropriate construction of a preconditioner. Consequently, we split the system into fluid variables and structure variables, which is not shown here to the convencience for the reader.

From this representation, we observe immediately that two terms are zero on the diagonal in the system matrix. This lack must be resolved when using a Block-Schur preconditioner. In (Janssen and Wick, 2010), the authors introduce artificial terms on the diagonal and weight them to reduce the influence on the mathematical model. However, this drastically reduces the performance of the iterative solver because the weighting factors influnce the condition number of the matrix and therefore the number of iteration steps. One idea to overcome this drawback was subject of investigation in (Richter, 2010). Here, the author use a partitioned solution algorithm to solve the monolithic problem. Another approach for a fast solver for monolithic problems was introduced in (Heil, 2004). Finally, other algorithms for solving fluid-structure interaction can be found in (Fernández and Moubachir, 2005; Barker and Cai, 2010).

4 Numerical results

We consider the numerical benchmark tests FSI 1, FSI 2 and FSI 3, which were proposed in (Bungartz and Schäfer, 2006). The configuration is sketched in Figure 1. New results can be found in (Bungartz and Schäfer, 2006; Turek et al., 2010; Degroote et al., 2010; Wick, 2011).

The first test case results in a stationary regime but is computed within a pseudo time stepping process with the implicit Euler scheme. The shifted Crank-Nicolson scheme was used for the both unsteady configurations FSI 2 and FSI 3.

Configuration

The computational domain has length $L = 2.5m$ and height $H = 0.41m$. The circle center is positioned at $C = (0.2m, 0.2m)$ with radius $r = 0.05m$. The elastic beam has length $l = 0.35m$ and height $h = 0.02m$. The right lower end is positioned at $(0.6m, 0.19m)$, and the left end is attached to the circle.

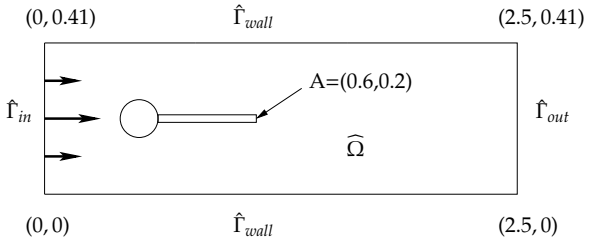

Figure 1: Flow around cylinder with elastic beam with circle-center $C = (0.2, 0.2)$ and radius $r = 0.05$.

Control points $A(t)$ (with $A(0) = (0.6, 0.2)$) are fixed at the trailing edge of the structure, measuring x- and y-deflections of the beam.

Boundary conditions

A parabolic inflow velocity profile is given on $\hat{\Gamma}_{in}$ by

$$v_f(0,y) = 1.5\bar{U}\frac{4y(H-y)}{H^2}, \quad \bar{U} = 0.2ms^{-1} \quad \text{(FSI 1)},$$
$$v_f(0,y) = 1.5\bar{U}\frac{4y(H-y)}{H^2}, \quad \bar{U} = 1.0ms^{-1} \quad \text{(FSI 2)},$$
$$v_f(0,y) = 1.5\bar{U}\frac{4y(H-y)}{H^2}, \quad \bar{U} = 2.0ms^{-1} \quad \text{(FSI 3)}.$$

On the outlet $\hat{\Gamma}_{out}$ the 'do-nothing' outflow condition ((Heywood et al., 1996)) is imposed which leads to zero mean value of the pressure at this part of the boundary. The remaining boundary conditions are chosen as in the CSM test cases.

Initial conditions

For the nonstationary tests one should start with a smooth increase of the velocity profile in time. We use

$$v_f(t;0,y) = \begin{cases} v_f(0,y)\frac{1-\cos(\frac{\pi}{2}t)}{2} & \text{if } t < 2.0s \\ v_f(0,y) & \text{otherwise.} \end{cases} \tag{14}$$

The term $v_f(0,y)$ is already explained above.

Quantities of comparison and their evaluation

1) x- and y-deflection of the beam at $A(t)$.

2) The forces exerted by the fluid on the whole body, i.e., drag force F_D and lift force F_L on the rigid cylinder and the elastic beam. They form a closed path in which the forces can be computed with the help of line integration. The formula is evaluated on the fixed reference domain $\hat{\Omega}$ and reads:

$$(F_D, F_L) = \int_{\hat{S}} \hat{J}\hat{\sigma}_{all}\hat{F}^{-T} \cdot \hat{n}\, d\hat{s} = \int_{\hat{S}(\text{circle})} \hat{J}\hat{\sigma}_f\hat{F}^{-T} \cdot \hat{n}_f\, d\hat{s} + \int_{\hat{S}(\text{beam})} \hat{J}\hat{\sigma}_f\hat{F}^{-T} \cdot \hat{n}_f\, d\hat{s}. \tag{15}$$

The quantities of interest for the time dependent test cases are represented by the mean value, amplitudes, and frequency of x- and y-deflections of the beam in one time period T of oscillations.

Parameters

We choose for our computation the following parameters. For the fluid we use $\varrho_f = 10^3 kgm^{-3}$, $\nu_f = 10^{-3}m^2s^{-1}$. The elastic structure is characterized by $\varrho_s = 10^4 kgm^{-3}$ (FSI 2) and $\varrho_s = 10^3 kgm^{-3}$ (FSI 1 and FSI 3), respectively, and $\nu_s = 0.4$. Furthermore, we use for the FSI 1 and FSI 2 test cases $\mu_s = 0.5 * 10^6 kgm^{-1}s^{-2}$ and for the FSI 3 test case $\mu_s = 2.0 * 10^6 kgm^{-1}s^{-2}$.

Table 1: Results for the FSI 1 benchmark with the biharmonic mesh motion model. The mean value and amplitude are given for the four quantities of interest: u_x, u_y, F_D, F_L.

DoFs	$u_x(A)[\times 10^{-5}m]$	$u_y(A)[\times 10^{-4}m]$	$F_D[N]$	$F_L[N]$
5445	2.3258	8.2397	14.6331	0.74577
20988	2.2808	8.1846	15.1434	0.74025
82368	2.2734	8.1751	15.3302	0.73982
326304	2.2703	8.1809	15.3776	0.74111

We observe the same qualitative behavior in each of our approaches for the quantities of interest ($u_x(A)$, $u_y(A)$, drag, and lift); these results are in agreement with (Turek et al., 2010).

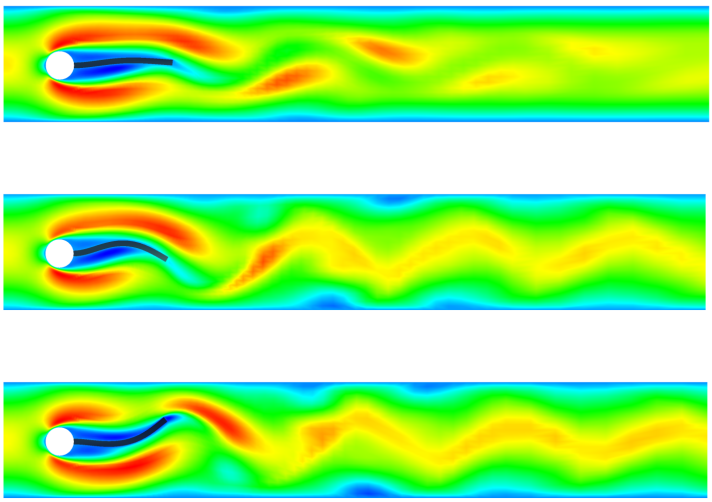

Figure 2: FSI 2: velocity field for three different time steps.

The velocity field for three different time steps is displayed in Figure 2. Here, we observe the Karman vortex street. The computed values of the FSI 1 test case are summarized in the Table 1. The results of the FSI 2 and the FSI 3 test are displayed in the Figures 3 and 4. The reference values are taken from (Turek et al., 2010). In general, to verify convergence with respect to space and time, at least three different mesh levels and time step sizes must be computed.

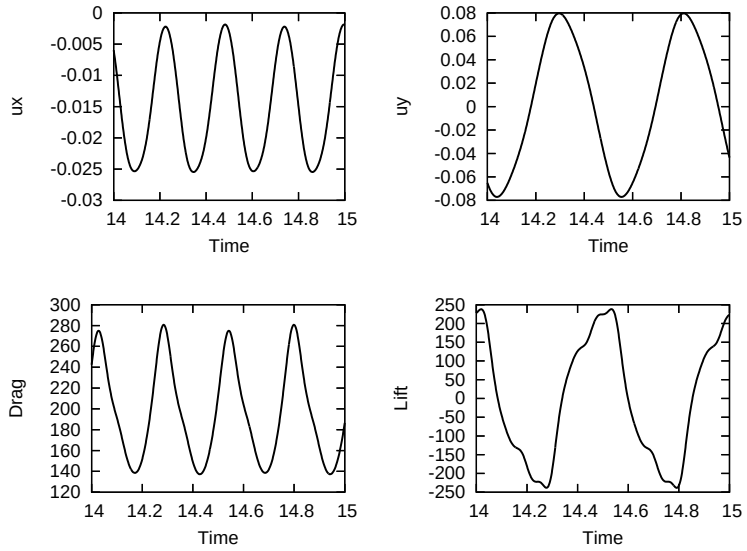

Figure 3: FSI 2. Top: the deflections of the beam, $u_x(A)$ and $u_y(A)$. Bottom: the drag and the lift computations over the path S of the cylinder and the interface between the fluid and the structure.

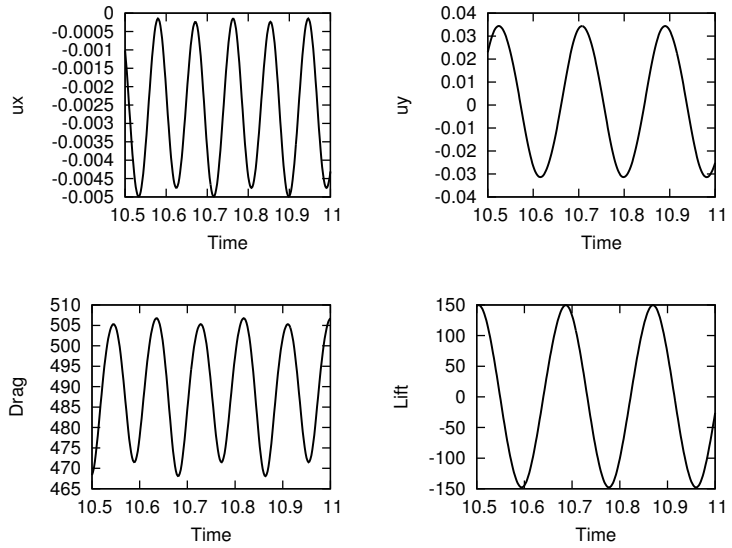

Figure 4: FSI 3. Top: the deflections of the beam, $u_x(A)$ and $u_y(A)$. Bottom: the drag and the lift computations over the path S of the cylinder and the interface between the fluid and the structure.

5 Conclusions

We presented a description of a monolithically-coupled fluid-structure interaction problem and its implementation using the deal.II software library. In upcoming works, we plan to implement efficient mesh refinement procedures and gradient based optimization routines. For these kind of problems, a closed monolithic formulation of the coupled problem, as presented in this work, is an indispensable requirement. Second, we plan to improve the solution process of the linear equation systems in each Newton step.

Apendix A: Library Information and Source Code Files

In this apendix, we describe the requirements to reproduce the results with the help of the provided source code. The implementation has been compiled with the deal.II 7.3.0 library. Specifically, the reader can create a subdirectory

```
1 step-fsi
```

in the deal.II examples folder that comes with the installation. Herein, the following files must be copied:

- The main source file with comments in which, for example, parameters might be changed to study other configurations and corresponding output data.

```
1 step-fsi.cc
```

- The grid to run the computation:

```
1 fsi.inp
```

- The standard simple Makefile of deal.II as used to run all other tuturial steps:

```
1 Makefile
```

  It is possible to change the path to the deal.II library in the Makefile. In the standard configuration, it is assumed that the reader works in an arbitrary directory in which the cc file has been copied. Assuming that deal.II is located in the home directory of the user, the following path can be found in the Makefile:

```
1 D = ~/deal.II
```

Apendix B: Features of the Implementation in deal.II

The implementation of the Problem 8 is realized in a similar fashion as most of the tutorial steps in deal.II. In the first part, we define some terms within three namespaces to keep the later implementation as clear as possible. We define the

```
1 namespace ALETransformations {...}
```

for tensors of the solution variables $\hat{u}, \hat{v}, \hat{p}, \hat{w}$ and their corresponding derivatives that become necessary for the Newton method. In the next namespace,

```
1 namespace NSEALE {...}
```

we declare the transformed fluid equations. The last namespace is used to organize the structure terms:


```
1 namespace StructureTermsALE {...}
```

Next, we introduce a class denoting nonhomogeneous Dirichlet boundary values:

```
1 class BoundaryParabolic {...}
```

After these preparations, we come to the main class of our implementation:

```
1 class FSIALEProblem {...}
```

An extensive description of this class can be found in the source file itself. In the following, we will briefly describe each function declared in this class. First, the constructor is used to initialize the finite elements and to specify their degree. Next, we define a function that deals with runtime parameters:

```
1 set_runtime_parameters () {...}
```

A possible extension of the provided source file, could be the following idea: to use a parameter handler object that reads these data from a file. Finally, the function

```
1 setup_system () {...}
```

is used to initialize the system matrix and several vectors that are later needed. So far, we have only prepared the basic framework that is a prequerisite to run the program. In the following, we treat the equations introduced in the theoretical part of this work, see Equation 8. We recall that we are supposed to solve at each Newton step a linear equation system. The ingredients are a left-hand-side, consisting of the Jacobian that is performed in

```
1 assemble_system_matrix () {...}
```

The corresponding right hand side is the residual of the semi-linear form that is computed in

```
1 assemble_system_rhs () {...}
```

Moreover, we set the initial boundary conditions of our problem in

```
1 set_initial_bc (...) {...}
```

In each Newton step, nonhomogeneous Dirichlet boundary conditions must be set to zero. Therefore, we declare a second function

```
1 set_newton_bc ()
```

where we replace all nonhomogeneous Dirichlet conditions by their corresponding homogeneous parts. The nonlinear system is treated by a Newton-like method,

```
1 newton_iteration (...)
```

that also includes some nice features, like a simple line search routine. Moreover, we check the improvement of the residual term in each Newton step. Depending on this check, we decide whether the system matrix needs to be rebuild or not. The probably most interesting function for possible future work is discussed in the following. Herein, we will solve the linear system (that arises in each Newton step) with a direct solver from UMFPACK:

```
1 solve () {...}
```

The following function is similar to many functions in the tutorial steps and manages the output of our results:

```
output_results (...) {...}
```

To determine the quality of our implementation, we need measure some physical quantities. In this study, we compute the deflections in the both principal directions:

```
compute_point_value (...) {...}
```

Additionally, we compute the forces (the drag and the lift) that act on the interface between the fluid and the structure, and the forces around the cylinder. These computations can be performed by line integration:

```
compute_drag_lift_fsi_fluid_tensor () {...}
```

Finally, we call the both aforementioned functions in

```
compute_functional_values () {...}
```

In the last function of the class,

```
run () {...}
```

the time stepping scheme, and all remaining routines, are performed. Finally, the main function is used to call the main class. It looks mostly like in almost all the other tutorial steps.

Apendix C: Running the Source Code for solving FSI 1,2,3

The provided programming code can be used to obtain the results presented in Section 4. By default, the FSI 1 configuration is computed. The other two configurations can be set up, first, in the

```
template <int dim>
class BoundaryParabolic
```

to change the inflow velocity. Increasing the inflow velocity leads to nonstationary behavior:

```
// FSI 1: 0.2; FSI 2: 1.0; FSI 3: 2.0
double inflow_velocity = 2.0e-1;
```

All remaining components are set up in the

```
set_runtime_parameters () {...}
```

function. Specifically, structure's density

```
// FSI 1 & 3: 1.0e+3; FSI 2: 1.0e+4
density_structure = 1.0e+3;
```

and the Lamé coefficient

```
// Structure parameters
// FSI 1 & 2: 0.5e+6; FSI 3: 2.0e+6
lame_coefficient_mu = 0.5e+6;
```

differ from case to case. To obtain nonstationary solutions, the time-stepping scheme should be of second order in time:


```
// Timestepping schemes
// BE, CN, CN_shifted
time_stepping_scheme = "BE";
```

Thus, one should choose CN or the shifted CN scheme for solving the FSI 2 and 3 problem. To reflect the dynamics of the system, altough we work with implicit time-stepping schemes without CFL condition, the time step should be sufficiently small:

```
// Timestep size:
// FSI 1: 1.0 (quasi-stationary)
// FSI 2: <= 1.0e-2 (non-stationary)
// FSI 3: <= 1.0e-3 (non-stationary)
timestep = 1.0;
```

Finally, reasonable maximal numbers of time steps (to corresponding end time values T) are

```
// Maximum number of timesteps:
// FSI 1: 25 , T= 25   (timestep == 1.0)
// FSI 2: 1500, T= 15  (timestep == 1.0e-2)
// FSI 3: 10000, T= 10 (timestep == 1.0e-3)
max_no_timesteps = 25;
```

With the help of these suggestions, all presented results of Section 4 can be computed with the provided source code.

Conclusions and ideas for further investigations with this program

The implementation makes use of some tools provided by deal.II. However, some features are novel in our code. Specifically, these are:

- The solution of a nonlinear time-dependent PDE with four blocks and seven components in total (2+2+2+1: for velocity, displacement, additional displacment, and pressure).
- The FESystem class in deal.II was extended to be able to deal with four finite elements.
- Implementation of a monolithically-coupled fluid-structure interaction problem with three types of nonlinearities:
  - convection term of the fluid,
  - nonlinear constitutive model of the structure problem,
  - nonlinear transformation rules induced by the ALE map.
- The geometry, the boundary conditions, and the initial conditions can be easily changed to run other configurations (pseudo stationary and unsteady, respectively). Specifically, large structural deformations can be simulated because of using the biharmonic fluid mesh motion model. For various examples (obtained by an analoguous deal.II code), we refer to (Wick, 2011) and (Wick, 2011).
- By omitting the structure terms (this can simply be realized by setting all material ids equal to 0 in the *.inp file), the user gets immediately a pure fluid solver because the transformation $\widehat{F}$ becomes the identity and then $\hat{J} = 1$. Then, all equations reduce to the well-known incompressible Navier-Stokes equations. By taking the benchmark grid for fluid flows (Schäfer and Turek, 1996) and adapting the initial conditions, one can have a try to reproduce these findings.

- The implementation of different time-stepping schemes in our code. It is well-known that the pure Crank-Nicolson scheme suffers from stability aspects for long-term computations and/or for rough initial data. A comparison of the pure Crank-Nicolson scheme with the shifted Crank-Nicolson scheme for the FSI 2 and FSI 3 test cases was already subject in (Wick, 2011). What does happen when using the backward Euler scheme for these examples?
- In the same manner, the finite elements for the spatial discretization can be changed. Since deal.II provides many different finite elements, one can easily change them. However, the inf-sup stability should be fulfilled or some appropriate stabilization must be added when using equal-order finite elements.

Possible future improvements of this program

The user of the source code is invited to have his/her own try for possible improvements. At present, we note these ideas:

- To replace the linear solver by an iterative solver, e.g. GMRES. Using a such solver, it is necessary to investigate theory and implementation using deal.II. However, the crucial issue is the construction of a preconditioner for the system matrix. The development of a Block-Schur preconditioner as in (Janssen and Wick, 2010) is one possibility but not the only one. To the best of our knowledge, the authors have already started further investigations to improve that approach.
- To implement efficient mesh refinement techniques; in particular for unsteady computations. For stationary settings of fluid-structure interaction problems, a first try with application in hemodynamics already exists (Wick, 2012).
- Solving a fluid-structure problem with many spatial unknowns (i.e., on a fine grid) and many time steps requires much more effort in computational power. For this reason, one could develop a parallel version of this code.

Acknowledgments

The author gratefully acknowledges Bärbel Janssen (University of Bern) and Guido Kanschat (Heidelberg University) and Wolfgang Bangerth (Texas A&M University) for fruitful discussions. Furthermore, the financial support by the DFG (Deutsche Forschungsgemeinschaft) and the HGS MathComp Heidelberg during my PhD time is acknowledged.

References

Z. Jianhai, C. Dapeng, Z. Shengquan, ALE finite element analysis of the opening and closing process of the artificial mechanical valve, Appl. Math. Mech. (2006) 403–412.

S. Piperno, C. Farhat, Paritioned procedures for the transient solution of coupled aeroelastic problems - part ii: energy transfer analysis and three-dimensional applications, Comput. Methods Appl. Mech. Engrg. 190 (2001) 3147–3170.

P. L. Tallec, J. Mouro, Fluid structure interaction with large structural displacements, Comput. Methods Appl. Mech. Engrg. 190 (2001) 3039–3067.

C. Figueroa, I. Vignon-Clementel, K. Jansen, T. Hughes, A coupled momentum method for modeling blood flow in three-dimensional deformable arteries, Comp. Methods Appl. Mech. Engrg. 195 (2006) 5685–5706.

N. D. D. Santos, J.-F. Gerbeau, J. Bourgat, A partitioned fluid-structure algorithm for elastic thin valves with contact, Comp. Methods Appl. Mech. Engrg. 197 (2008) 1750–1761.

F. Nobile, C. Vergara, An effective fluid-structure interaction formulation for vascular dynamics by generalized Robin conditions, SIAM J. Sci. Comput. 30 (2008) 731–763.

J. Vierendeels, K. Dumont, P. Verdonck, A partitioned strongly coupled fluid-structure interaction method to model heart valve dynamics, J. Comp. Appl. Math. (2008).

J. Hron, Fluid structure interaction with applications in biomechanics, Ph.D. thesis, Charles University Prague, 2001.

J. Hron, S. Turek, A monolithic FEM/Multigrid solver for ALE formulation of fluid structure with application in biomechanics, volume 53, Springer-Verlag, pp. 146–170.

M. Fernández, J.-F. Gerbeau, Algorithms for fluid-structure interaction problems, volume 1 of Formaggia et al. (2009), pp. 307–346.

H.-J. Bungartz, M. Schäfer, Fluid-Structure Interaction: Modelling, Simulation, Optimization, volume 53 of *Lecture Notes in Computational Science and Engineering*, Springer, 2006.

T. Richter, T. Wick, Finite elements for fluid-structure interaction in ALE and fully Eulerian coordinates, Comp. Methods Appl. Mech. Engrg. 199 (2010) 2633–2642.

H.-J. Bungartz, M. Mehl, M. Schäfer, Fluid-Structure Interaction II: Modelling, Simulation, Optimization, Lecture Notes in Computational Science and Engineering, Springer, 2010.

T. Wick, Fluid-structure interactions using different mesh motion techniques, Comput. Struct. 89 (2011) 1456–1467.

W. Wall, S. Genkinger, E. Ramm, A strong coupling partitioned approach for fluid-structure interaction with free surfaces, Computers and Fluids 36 (2007) 169–183.

H. Matthies, R. Niecamp, J. Steindorf, Algorithms for strong coupling procedures, Comp. Methods Appl. Mech. Engrg 195 (2006) 2028–2049.

T. Tezduyar, S. Sathe, K. Stein, Solution techniques for the fully discretized equations in computation of fluid-structure interaction with space-time formulations, Comp. Methods Appl. Mech. Engrg. 195 (2006) 5743–5753.

U. Küttler, W. A. Wall, The dilemma of domain decomposition approaches in fluid-structure interactions with fully enclosed incompressible fluids, volume 60 of *Domain decomposition methods in science and engineering XVII*, Springer, Berlin, pp. 575–582.

D. Mok, W. Wall, Partitioned analysis schemes for the transient interaction of incompressible flows and nonlinear flexible structures, Trends in Computational Structural Mechanics, CIMNE, Barcelona.

S. Deparis, M. Discacciati, G. Fourestey, A. Quarteroni, Fluid-structure algorithms based on Steklov-Poincaré operators, Comp. Methods Appl. Mech. Engrg 195 (2006) 5797–5812.

R. Becker, H. Kapp, R. Rannacher, Adaptive finite element methods for optimal control of partial differential equations: basic concepts, SIAM J. Optim. Control 39 (2000) 113–132.

R. Becker, R. Rannacher, An optimal control approach to error control and mesh adaptation in finite element methods, Acta Numerica 2001, Cambridge University Press, a. iserles edition, pp. 1–102.

K. van der Zee, E. van Brummelen, R. de Borst, Goal-oriented error estimation for Stokes flow interacting with a flexible channel, International Journal of Numerical Methods in Fluids 56 (2008) 1551–1557.

T. Richter, Goal-oriented error estimation for fluid-structure interaction problems, Comp. Methods Appl. Mech. Engrg. 223-224 (2012) 38–42.

T. Wick, Goal-oriented mesh adaptivity for fluid-structure interaction with application to heart-valve settings, Arch. Mech. Engrg. 59 (2012) 73–99.

T. Wick, Adaptive Finite Element Simulation of Fluid-Structure Interaction with Application to Heart-Valve Dynamics, Ph.D. thesis, University of Heidelberg, 2011.

P. Causin, J.-F. Gerbeau, F. Nobile, Added-mass effect in the design of partitioned algorithms for fluid-structure problems, Comput. Methods Appl. Mech. Engrg. 194 (2005) 4506–4527.

J. Donéa, P. Fasoli-Stella, S. Giuliani, Lagrangian and Eulerian finite element techniques for transient fluid-structure interaction problems, in: Trans. 4th Int. Conf. on Structural Mechanics in Reactor Technology, p. Paper B1/2.

O. Ghattas, X. Li, A variational finite element method for stationary nonlinear fluid-solid interaction, J. Comput. Phys. 121 (1995) 347–356.

C. Hirt, A. Amsden, J. Cook, An arbitrary Lagrangian-Eulerian computing method for all flow speeds, J. Comput. Phys. 14 (1974) 227–253.

T. Hughes, W. Liu, T. Zimmermann, Lagrangian-Eulerian finite element formulation for incompressible viscous flows, Comput. Methods Appl. Mech. Engrg. 29 (1981) 329–349.

B. Helenbrook, Mesh deformation using the biharmonic operator, Int. J. Numer. Methods Engrg. (2001) 1–30.

S. Turek, Efficient solvers for incompressible flow problems, Springer-Verlag, 1999.

V. Girault, P.-A. Raviart, Finite Element method for the Navier-Stokes equations, Number 5 in Computer Series in Computational Mathematics, Springer-Verlag, 1986.

F. Fernández, M. Moubachir, A Newton method using exact Jacobians for solving fluid-structure coupling, Comput. Struct. 83 (2005) 127–142.

M. Heil, An efficient solver for the fully coupled solution of large-displacement fluid-structure interaction problems, Comput. Methods Appl. Mech. Engrg. 193 (2004) 1–23.

S. Badia, Q. Quaini, A. Quarteroni, Splitting methods based on algebraic factorization for fluid-structure interaction, SIAM J. Sci. Comput. 30 (2008) 1778–1805.

T. Richter, A monolithic multigrid solver for 3d fluid-structure interaction problems, SIAM J. Sci. Comput. (2010). Submitted.

T. A. Davis, I. S. Duff, An unsymmetric-pattern multifrontal method for sparse LU factorization, SIAM J. Matrix Anal. Appl. 18 (1997) 140–158.

W. Bangerth, T. Heister, G. Kanschat, Differential Equations Analysis Library, 2012.

J. Wloka, Partielle Differentialgleichungen, B. G. Teubner Verlag, Stuttgart, 1982.

P. Ciarlet, P.-A. Raviart, A mixed finite element method for the biharmonic equation, Mathematical Aspects of Finite Elements in Partial Differential Equations, Academic Press, New York, pp. 125–145.

T. Wick, Stability estimates and numerical comparison of second order time-stepping schemes for fluid-structure interactions, in: Numerical Mathematics and Advanced Applications 2011, ENUMATH 2011 in Leicester, UK.

A. Barker, X.-C. Cai, Scalable parallel methods for monolithic coupling in fluid-structure interaction with application to blood flow modeling, J. Comput. Phys. 229 (2010) 642–659.

B. Janssen, T. Wick, Block preconditioning with Schur complements for monolithic fluid-structure interactions, in: J. Pereira, A. Sequeira (Eds.), ECCOMAS CFD 2010, Lisbon.

B. Janssen, G. Kanschat, Adaptive multilevel methods with local smoothing for H^1- and H^{curl}-conforming high order finite element methods, SIAM J. Sci. Comput (2011). To be published.

S. Turek, J. Hron, M. Madlik, M. Razzaq, H. Wobker, J. Acker, Numerical simulation and benchmarking of a monolithic multigrid solver for fluid–structure interaction problems with application to hemodynamics, Technical Report, Fakultät für Mathematik, TU Dortmund, 2010. Ergebnisberichte des Instituts für Angewandte Mathematik, Nummer 403.

J. Degroote, R. Haelterman, S. Annerel, P. Bruggeman, J. Vierendeels, Performance of partitioned procedures in fluid-structure interaction, Comput. Struct. (2010) 446–457.

J. G. Heywood, R. Rannacher, S. Turek, Artificial boundaries and flux and pressure conditions for the incompressible Navier-Stokes equations, International Journal of Numerical Methods in Fluids 22 (1996) 325–352.

M. Schäfer, S. Turek, Flow Simulation with High-Performance Computer II, volume 52 of *Notes on Numerical Fluid Mechanics*, Vieweg, Braunschweig Wiesbaden.

L. Formaggia, A. Quarteroni, A. Veneziani, Cardiovascular Mathematics: Modeling and simulation of the circulatory system, Springer-Verlag, Italia, Milano, 2009.

